Original Article

Utility of CT in detecting and monitoring subphrenic jujube pits: a retrospective cross-sectional study of clinical cases and *ex vivo* experiments

Luwen Hao[#], Qiuxia Wang[#], Xuemei Hu, Zhen Li, Daoyu Hu, Yaqi Shen

Department of Radiology, Tongji Hospital, Tongji Medical College, Huazhong University of Science and Technology, Wuhan, China

Contributions: (I) Conception and design: Y Shen; (II) Administrative support: Z Li, D Hu; (III) Provision of study materials or patients: X Hu; (IV) Collection and assembly of data: L Hao, Q Wang; (V) Data analysis and interpretation: L Hao, Q Wang, Y Shen; (VI) Manuscript writing: All authors; (VII) Final approval of manuscript: All authors.

[#]These authors contributed equally to this work and should be considered as co-first authors.

Correspondence to: Yaqi Shen. Department of Radiology, Tongji Hospital, Tongji Medical College, Huazhong University of Science and Technology, 1095 Jiefang Avenue, Qiaokou District, Wuhan 430030, China. Email: yqshen@hust.edu.cn.

Background: Subphrenic jujube foreign body can cause perforation, abscess, peritonitis and other complications. Computed tomography (CT) is considered to be a sensitive tool for small or faintly opaque foreign body (e.g., jujube pits, toothpicks, fish bones, acrylics and plastics) detection. The present study aimed to investigate the clinical and imaging features of subphrenic jujube pits and explore the potential of CT for detecting and monitoring subphrenic jujube pits.

Methods: Patients with subphrenic jujube pits who were treated at our institution were retrospectively reviewed along with published studies. A total of 10 types of commercially available jujube pits were analyzed with CT, then another 40 jujube pits (≥2.5 cm) were randomly selected and soaked in a series of solutions to mimic the gastrointestinal tract processes, following which CT was performed at serial time points with conventional and dual-energy protocols.

Results: All jujube pits could be detected by CT, presenting spindle-shape high-density. The length of jujube pits based on clinical cases and that of the commercially available types were 1.38 to 3.50 cm and 1.35 to 3.95 cm, respectively. After analysis, the mean attenuation values derived from the clinical cases [77.67 Hounsfield unit (HU), range: −89.92 to 153.13 HU, SD 64.70 HU] were higher than those of the 10 commercially available types of jujube pits in boiled (73.57 HU, range: 2.29 to 94.96 HU, SD 20.48 HU) and raw state (−274.28 HU, range: −400.12 to −168.12 HU, SD 72.75 HU); statistically significant differences were found in mean attenuation values between raw jujube pits and boiled jujube pits ($P<0.05$). After soaking, the radiodensity of raw jujube pits showed an upward trend over immersion time, and water (-hydroxyapatite) overlay images enhanced the visualization of jujube pit water content as the percentage of blue area increased over time.

Conclusions: CT plays an important role in evaluating and tracing subphrenic jujube pits.

Keywords: Computed tomography (CT); gastrointestinal foreign bodies; jujube pits; *ex vivo* experiment; acute abdomen

Submitted Jan 29, 2022. Accepted for publication Aug 03, 2022.
doi: 10.21037/qims-22-53
View this article at: https://dx.doi.org/10.21037/qims-22-53

Introduction

Dried jujube (Ziziphus jujuba Mill) fruits have been used in food, flavoring, and pharmaceuticals for thousands of years (1,2). Jujube available in the market differs in terms of production area and cultivar (3). The pulp and pit cannot be easily separated, which leads to involuntary and accidental deglutition of jujube pits (4). Most jujube pits are embedded in the esophagus and can be detected and removed by endoscopy (5); hence, subphrenic jujube pits are relatively rare. A few studies have reported subdiaphragmatic jujube pit foreign bodies, to our knowledge, totaling 45 patients with jujube pits located in the subphrenic digestive tract (stomach, n=20; small intestine, n=22; colon, n=1; rectum, n=2) were reported worldwide (5-10).

Jujube pit foreign bodies can cause adverse events, such as obstruction, perforation, abscesses, peritonitis, or systemic sepsis due to their two sharp heads (6,8,10,11). The European Society of Gastrointestinal Endoscopy and American Society for Gastrointestinal Endoscopy pointed out that foreign bodies greater than 2.5 cm in diameter were unlikely to pass through the pylorus (12,13). It is still unclear whether complications are related to the length or width of jujube pits.

In most clinical scenario, clear information on foreign body ingestion is rarely available, even with adult patients. Patients with foreign bodies impacted in the subphrenic gastrointestinal tract generally present with nonspecific clinical manifestations mimicking various inflammatory conditions (14,15). Thus, endoscopy is not the initial examination in this clinical situation. However, plain radiographs often fail to recognize wooden foreign bodies (e.g., jujube pit and toothpick) (12). Computed tomography (CT) is considered to be a sensitive tool for foreign body detection, and the sensitivity of CT in detecting faintly opaque objects is higher than that of plain radiographs (16). Additionally, dual-energy CT is a promising tool for the evaluation of non-traumatic acute abdomen, with its ability to characterize materials (17). Two types of reconstruction images acquired by DECT have been widely used: virtual monoenergetic images are helpful to differential diagnosis of tumors (18,19), and material decomposition images can quantity bone mineral density, liver iron content, and liver fat content (20,21). Dual-energy CT may help to characterize and distinguish different types of subphrenic foreign bodies, such as illegal intra-corporeal packets of cocaine and non-ferromagnetic projectiles (22,23). Moreover, the guideline emphasized that CT scans were recommended for all patients with suspected perforation or other complications (12).

The jujube pit appeared as a shuttle with two sharp points or a ring depending on the orientation of the CT images, according to a recent study (8). However, the CT performance for the diagnosis of subphrenic jujube pits is uncertain. A comprehensive study is necessary to investigate the performance of CT in identifying jujube pits.

Furthermore, it is still a challenge to guide the clinical management of subphrenic jujube pits due to a lack of deeper consensus regarding the management of sharp-pointed foreign bodies (24).

Therefore, this study aimed to (I) illustrate the clinical and CT features of subphrenic jujube pit foreign bodies and (II) determine whether dual energy-CT can differentiate jujube pits at different sites over time in gastrointestinal-process-mimicking phantom experiments. In general, the purpose of this research was to improve the understanding of sharp, faintly radiopaque, and subphrenic jujube pit foreign bodies and investigate the role of CT in diagnosing subphrenic jujube pit foreign bodies. We present the following article in accordance with the STROBE reporting checklist (available at https://qims.amegroups.com/article/view/10.21037/qims-22-53/rc).

Methods

Patients and clinical data collection

The study was conducted in accordance with the Declaration of Helsinki (as revised in 2013). Institutional ethics board of Tongji Hospital approved this retrospective cross-sectional study (No. TJ-IRB20211142), and informed consent was waived because of the retrospective nature of the study. Patients who visited Tongji hospital, between January 2014 and July 2021 with CT reports suggesting a subphrenic foreign body were retrospectively reviewed. Inclusion criteria were patients with subphrenic jujube pits confirmed by surgery, endoscopy, or jujube pits found in stool during clinical follow-up. Exclusion criteria were patients with non-jujube pit foreign bodies by typical imaging features (e.g., fish bone, toothpick and metal foreign body) on CT images (25-28) or identified by medical records, insufficient data, and those transferred to another hospital.

Literatures were searched from January 1950 through December 2021 in PubMed using the keywords “foreign bodies” and “jujube pit” and cases of subphrenic jujube

pits were enrolled for comparison with clinical cases from our institution (5-10) (Table S1). Jujube pit cases from our institution and the previously published cases were separately defined as the present study group and the reference report group, respectively.

Clinical data of all enrolled patients for analysis included age, sex, complaints (e.g., abdominal pain and vomiting), history of foreign body ingestion, laboratory variables, physical signs, and treatment modality.

CT examination and image analysis

CT technique

CTs were randomly used in clinic patients. CT scans were obtained using helical CT technology and our clinical abdominal imaging protocol. The detailed protocols and vendors of CTs for enrolled patients in present study were retrospectively reviewed in Table S2.

Qualitative CT image analysis

Qualitative CT image analysis were conducted with the present study group due to the image available. In addition to the routine abdominal window setting, a review of images in multiple window settings is indispensable for extraluminal air and foreign bodies (29). Axial images with attached multiplanar reformation tools were available (14) for two radiologists (QW and YS, 8 and 11 years of experience in Abdominal imaging, respectively). They had extensive experience in diagnosis of gastrointestinal foreign bodies, and aware patients were all with foreign body but were blinded to the clinical details; the following main analytical contents were independently assessed: (I) identify the presence of jujube pit, including location, number, and shape; (II) evaluate foreign body-related gastrointestinal injury and complications based on digestive tract wall thickening, intestinal dilation, extraluminal air, ascites, and fat stranding. If there is a discrepancy between the two radiologists, they would have a discussion and reach a consensus.

Quantitative CT image analysis

In addition to the visual evaluation, quantitative CT image analysis were conducted by two radiologists (QW and YS) after they had been trained for jujube pit measurements using ImageJ (RRID:SCR_003070), including the following parameters: (I) size: length and width of the jujube pits were measured. (II) Region of interest (ROI) measurements: the largest jujube pit section was defined as a ROI in the image; ROI measurements including mean-HU [the mean value of the ROI attenuation coefficient in Hounsfield units (HUs)] and max-HU (the maximum ROI attenuation coefficient in HUs) were performed on multiplanar reconstructed images revealing the largest section of the jujube pits (Figure S1). To ensure reliability and reproducibility, the two radiologists performed all the quantitative measurements separately on a PACS workstation. The measurement data were used to assess the intra-reader reliability using the intraclass correlation coefficient (ICC) and further averaged as the final results of the quantitative parameters.

Ex vivo study

Given the variability among species, jujube pits were obtained from ten commercially available types of jujube fruits among China. To mimic different clinical scenarios, raw and boiled status [ingested as food flavoring in the form of soup and congee (8)] of jujube pits were explored. And jujube pits were further soaked into different liquid conditions to mimic the various GI tract environment.

CT study of commercially available jujube pits in air

Ten kinds of dried jujube fruits were collected and numbered as S1–S10 (Table S3). Each type contained five dried jujube fruits. All jujube pits (n=50) were fixed on a plastic plate and performed with CT scans in air, first in raw state, followed by boiled. The CT scanning parameters were the same as those used in our clinical abdominal imaging protocol. Axial slices of 1.25-mm thickness were acquired. Size and radiodensity were measured by the two radiologists (QW and YS) using the same methods (mentioned in Quantitative CT image analysis, Figure S1). The measurement differences between the raw and boiled jujube pits were compared.

Ex vivo simulation experiment of jujube pits immersed in digestive tract fluid

After analyzing the initial data (Figure S2 and Table S3), only jujube pits longer than 2.5 cm were chosen for further mimic phantom study, including 20 raw and 20 boiled jujube pits together. They were then equally divided into five groups and soaked in five different solutions: double distilled water, saline, commercially available simulated gastric fluid, commercially available simulated intestinal fluid, and mixed solution (30). Double distilled water was used as a control, while the other four solutions

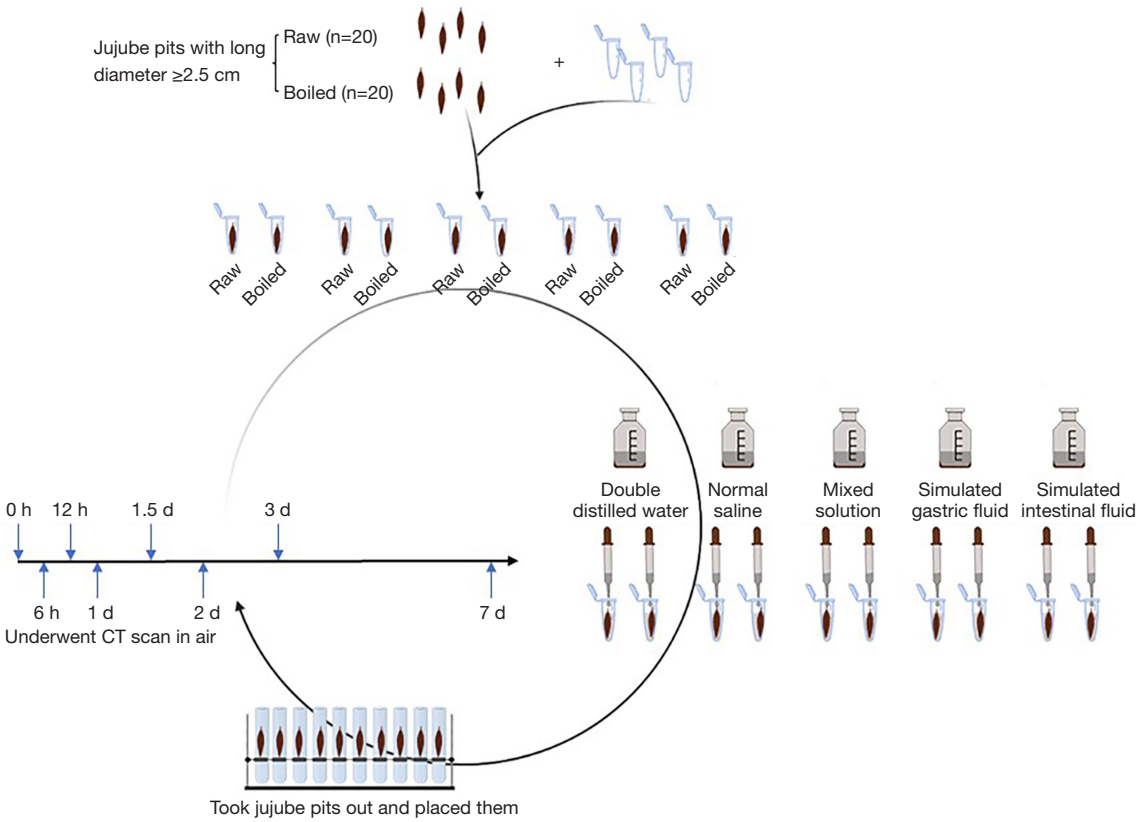

Figure 1 Chart of the *ex vivo* simulation model of the digestive tract fluid marinating jujube pits. Raw and boiled jujube pits were randomly divided into five separate groups. Jujube pit was traced and scanned at 0 hour (h), 6 h, 12 h, 1 day (d), 1.5 d, 2 d, 3 d, 7 d of immersion. The figure is created via Photoshop application (RRID: SCR_014199). CT, computed tomography.

simulated the liquid conditions of the gastrointestinal tract and extracellular fluid. A mixed solution mimicking the human biological processes during food digestion was also used, in a way that jujube pits were soaked in simulated gastric fluid for the first 4 h followed by immersion in simulated intestinal fluid. CT scans (Revolution CT, GE healthcare, Milwaukee, WI, USA.) were performed on all the samples before and after immersion at 6 h, 12 h, 18 h, 1 d, 1.5 d, 2 d, 3 d, and 7 d, including conventional helical series at 120 kVp and dual-energy CT series (gemstone spectral imaging CT scan) (*Figure 1*), and 0.625-mm-thick contiguous slices were acquired from both series and stored as DICOM images for further processing. For the dual-energy CT series, monochromatic 40 keV images, water (-hydroxyapatite) images, and water (-iodine) images were reconstructed on the gemstone spectral imaging viewer. The images were evaluated by the two radiologists (QW and YS), including measurements of density and water content as well as visual assessments of density and water content (Figure S1). Mean-HU changing trends of JPs in monochromatic 40 keV images over immersion time were analyzed.

Statistical analyses

Categorical data are presented as percentages, and continuous data are presented as mean ± standard deviation (SD) or upper and lower limits. Clinical characteristics and details of jujube pits from present study group and reference report group were compared using the Pearson chi-square test, Fisher exact test, or Mann-Whitney test as appropriate; data not available were not included in the comparison. Differences in CT measurements between jujube pits from commercially available types and clinical cases in our institution were assessed using one-way analysis of variance; post-hoc multiple comparisons were performed using the Tukey-Kramer honestly significant difference test. T-tests were applied to compare the blue area ratio between raw

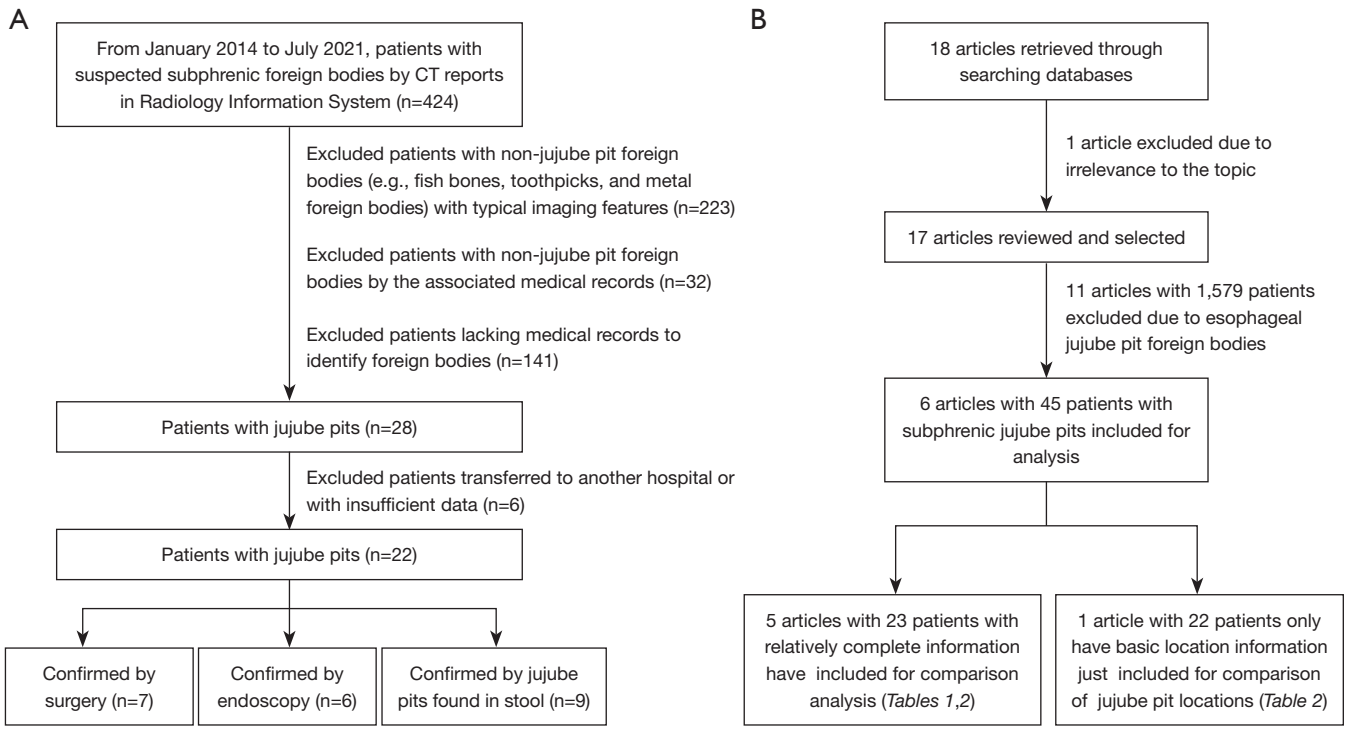

Figure 2 Flow chart of the study population. (A) Chart shows inclusion and exclusion criteria of patients in the present study group. (B) Chart shows the searching strategy and inclusion criteria of patients in the reference reported group for comparative analysis.

and boiled jujube pits. Intra-reader agreement was assessed using ICC. All statistical analyses were performed using SPSS (RRID:SCR_002865, version 23.0).

Results

Clinical cases

A total of 22 patients (9 men and 13 women, mean age 49.55±25.91 years, range, 1–85 years) were included in the present study group (*Figure 2A*) and 45 patients were enrolled in the reference reported group (*Figure 2B*) (5-10). Among the 45 patients, 23 patients (6-10) included in the comparison of clinical characteristics and details of jujube pits. Due to a lack of critical data, analyses of other 22 patients were only conducted on location of jujube pits (5).

Clinical characteristics

The clinical characteristics of the patients and the results of the statistical comparisons between the present study and the reference reports are summarized in *Table 1*.

No significant differences were observed in age, sex, dietary history, and inpatient treatment between the two groups. The age distribution tended to be middle-aged in both groups. The sex ratio was almost balanced. More than half of cases were not able to provide an history of foreign body ingestion.

Patients with positive symptoms, positive physical signs (fever, abdominal tenderness, and rebound tenderness) and perforation were significantly more frequent in the reference group (positive symptoms, 81.82% *vs.* 100%, P=0.049; positive physical signs, 63.64% *vs.* 100%, P=0.001; perforation, 50% *vs.* 100%, P<0.001). Abdominal pain, nausea, and vomiting were common clinical signs. However, the symptom of two patients with rectal perforation in reference reported group were untypical.

All cases in the reference reported group were inpatients. Among them, 21 (91.30%) patients showed signs of inflammation with elevated white blood cell count, procalcitonin, and C-reactive protein. In the present study group, the laboratory findings of many outpatients were not traceable. The patients in the present study group received both outpatient and inpatient treatment, including surgery (*Figure 3*), endoscopy (*Figure 4*), conservative treatment, or non-intervention with follow-up (*Figure 5*). For the

Table 1 Comparison of enrolled patients' clinical characteristics with reference reports

Parameters	Present study	Reference reported[†]	All	P value[‡]
Numbers of patients	22	23	45	
Age (years), n (%)				0.207
<6	4 (18.18)	2 (8.70)	6 (13.33)	
6–18	–	–	–	
19–50	2 (9.09)	3 (13.04)	5 (11.11)	
>50	16 (72.73)	18 (78.26)	34 (75.56)	
Gender, n (%)				0.295
Male	9 (40.91)	13 (56.52)	22 (48.89)	
Female	13 (59.09)	10 (43.48)	23 (51.11)	
Dietary history, n (%)				0.862
Have relevant information[§]	9 (40.91)	10 (43.48)	19 (42.22)	
Naught	13 (59.09)	13 (56.52)	26 (57.78)	
Symptom, n (%)				0.049*
Abnormal[¶]	18 (81.82)	23 (100.00)	41 (91.11)	
Asymptomatic	4 (18.18)	–	4 (8.89)	
Physical sign, n (%)				0.001*
Abnormal[¶]	14 (63.64)	23 (100.00)	37 (82.22)	
Normal	8 (36.36)	–	8 (17.78)	
Laboratory findings[††], n (%)				/
Abnormal[¶]	7 (31.82)	21 (91.30)	28 (62.22)	
Normal	6 (27.27)	2 (8.70)	8 (17.78)	
Not available	9 (40.91)	–	9 (20.00)	
Complication, n (%)				<0.001*
Perforation	11 (50.00)	23 (100.00)	34 (75.56)	
Non-perforation	11 (50.00)	–	11 (24.44)	
Inpatient treatments, n (%)				0.125
Endoscopic removal	–	1 (4.35)	1 (2.22)	
Surgical removal	7 (31.82)	19 (82.61)	26 (57.78)	
Conservative treatments[‡‡]	3 (13.64)	3 (13.04)	6 (13.33)	
Nontherapeutic and follow-up	2 (9.09)	–	2 (4.44)	
Outpatient treatments[††], n (%)				/
Endoscopic removal	5 (22.73)	–	5 (11.11)	
Conservative treatments and follow-up	3 (13.64)	–	3 (6.67)	
Nontherapeutic and follow-up	2 (9.09)	–	2 (4.44)	

[†], A total of 5 articles with 23 patients enrolled in reference reported group, including Ma *et al.*, 2021 (6), Liu *et al.*, 2020 (7), Li *et al.*, 2019 (8), Li *et al.*, 2017 (9), Lavers *et al.*, 1964 (10). [‡], P value of comparation between present study group and reference reported group. [§], have relevant information: awareness of jujube pit ingestion or recall of jujube ingestion. [¶], abnormal symptoms: common signs of gastrointestinal foreign bodies like abdominal pain, nausea and vomiting. Abnormal physical signs: common signs of gastrointestinal foreign bodies like fever, abdominal tenderness and tenderness and rebound tenderness. Abnormal laboratory findings: elevated inflammation indicators: white blood cell counts, procalcitonin, and C-reactive protein. [††], some patients were not mentioned, for some parameters such as: laboratory findings and outpatient treatments. These data were not compared. [‡‡], one patient underwent conservative treatment after failure of endoscopic removal. "–", defined as the number of the relative cell is 0. "/", defined as comparation of the relative parament was not done. *, a P value of <0.05 indicates a significant difference.

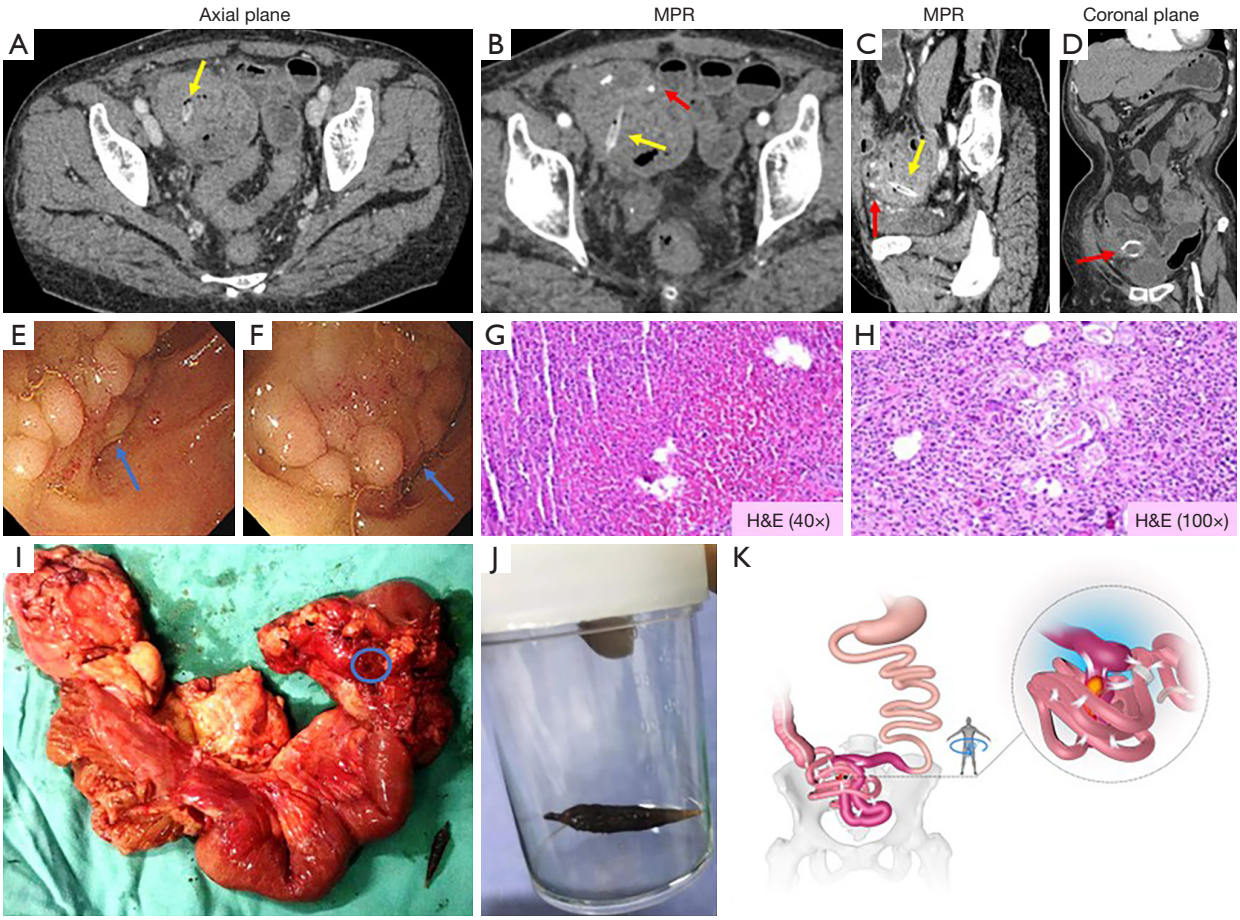

Figure 3 Illustration of small bowel perforation caused by a jujube pit. A 70-year-old woman visited the clinic and presented with unprovoked mild pain in the right lower quadrant, nausea, and vomiting for a month. She had been treated for appendicitis at a local hospital without remission. She had small bowel resection because of gastrointestinal stromal tumor (ileum, high-risk) 18 months ago. Axial CT images revealed a high-density jujube pit in the mass near the ileocecal region (A, yellow arrow), which was visualized as a typical shuttle shape on MPR images (B,C, yellow arrow). MPR images also revealed that the long axis of the foreign body was perpendicular to the anastomosis (B,C, red arrow). Elliptical shape of the anastomosis (D, red arrow) is better visualized on coronal image. Enteroscopy revealed a bulging lesion (E,F, blue arrow) in the terminal ileum that could not pass through the stenosis. Biopsy confirmed that the mass was an abscess (G: H&E, ×40); (H: H&E, ×100). The patient eventually underwent surgery. Intraoperative exploration revealed a hard jujube pit (I,J) inside of a mass in the ileocecal region and a perforation (I, blue circle) of the serous membrane. Schematic of the occurrence of foreign body perforation caused by postoperative adhesions (K). Panel (K) is created via Cinema 4D-remodelling software (MAXON Computer GmbH) and Photoshop software (RRID: SCR_014199). MPR, multiplanar reconstructions; CT, computed tomography; H&E, hematoxylin and eosin.

inpatients in both groups, surgical removal is the most common treatment.

In the present study group, 19 (86.36%) patients had acute onset, and the other 3 (13.64%) patients presented with subacute or chronic disease. A total of 4 (8.89%) patients in the two groups have prolonged disease course (1.5–48 months) as jujube pits had not been detected and removed timely.

Roles of CT in detecting and tracing subphrenic jujube pits

In both groups, all jujube pits could be detected by CT. Except details of CT detection in 24 patients were not available (*Table 2*), the detection rate on the initial imaging

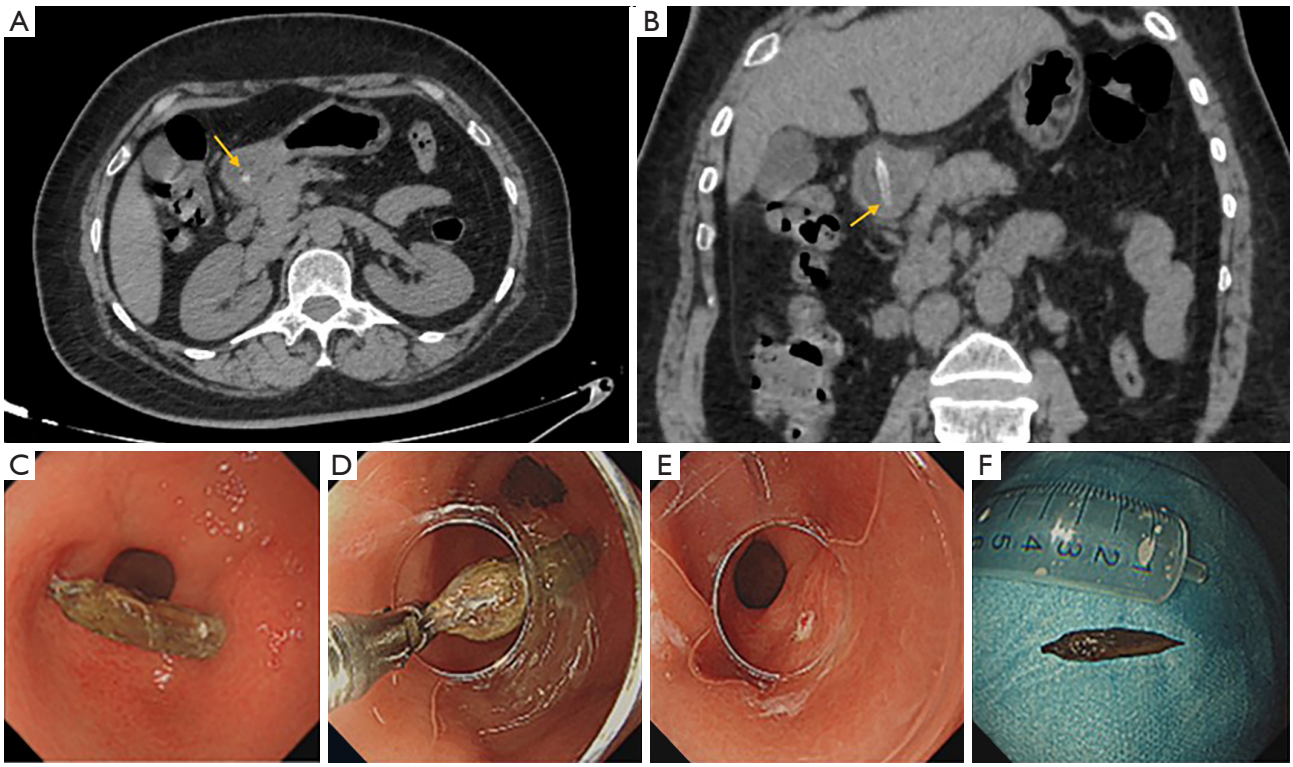

Figure 4 A jujube pit impacted in the gastric antrum. A 53-year-old woman presented with complaints of abdominal pain for seven hours without a history of jujube pit ingestion. CT suspected a jujube pit foreign body impacted in the gastric antrum with two sharp endpoints. Endoscopic findings were consistent with the CT findings, and the foreign body was removed. (A) Axial images demonstrate a dot high-density shadow (yellow arrow) in the gastric antrum, which can be easily missed. (B) MPR images clearly showed a jujube pit (yellow arrow) with both tips stuck under the mucosa. (C) Endoscopic visualization of a jujube pit in the gastric antrum. (D) Extraction of the jujube pit with foreign body forceps. (E) Small ulcerated foci are seen after jujube pit was removed. (F) Extracted jujube pit. MPR, multiplanar reconstructions; CT, computed tomography.

reports were different in two groups (present study n=24, 96%; reference report group n=14, 66.67%). Jujube pits could be found anywhere along the gastrointestinal tract, small intestine is the most common site (n=35, 50.00%). There were no statistically significant differences between the location distributions of the two groups. Size details of most patients were lack in reference report group. In present group, larger jujube pits (≥2.5 cm) were either lodged in or perforated the gastrointestinal tract without exception on CT images. Patients who did not undergo surgery or endoscopy to remove the jujube pits needed CT scans to monitor them until they were passed with stool (*Figure 5*).

CT features of jujube pits

In total, all 25 jujube pits were detected by CT in 22 patients in the present study group when reviewing. The CT characteristic of jujube pit is high-density shaped like a shuttle with two sharp ends. The density is heterogeneous, with a higher density margin, and the density decreases inward. Low-density hollow areas of different sizes were detected in 13 Jujube pits. Mean-HU ranged from −89.92 to 153.13 HU and max-HU ranged from 156 to 315 HU (*Figure 6A*). Intra-reader agreement was excellent for ROI measurements of mean-HU and max-HU (ICC =0.987, P<0.001; and ICC =0.980, P<0.001, respectively). The length and width of the jujube pits ranged from 1.38 to 3.50 cm and 0.47 to 0.71 cm, respectively (*Figure 6B*). Intra-reader agreement was excellent for length and width (ICC =0.991, P<0.001; and ICC =0.876, P<0.001, respectively).

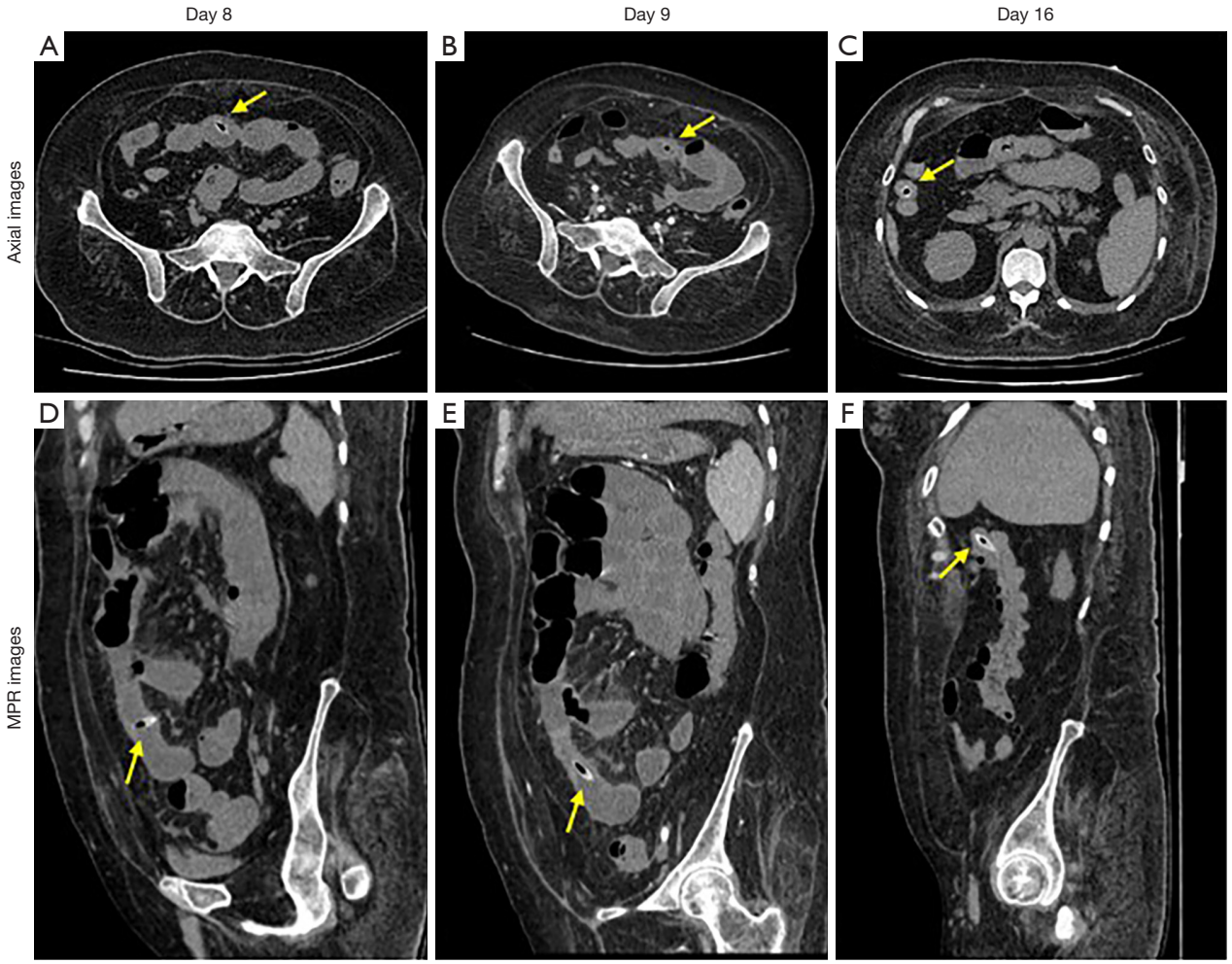

Figure 5 CT monitoring intestinal perforation caused by a jujube pit. A 51-year-old woman presented with complaints of abdominal pain for one week without a history of jujube pit ingestion. Abdominal examination revealed abdominal tenderness and rebound tenderness. CT revealed a jujube pit foreign body penetrating the intestinal wall, causing intestinal perforation. The patient was given conservative treatment because of contraindications, such as cardiac insufficiency and diabetes. The jujube pit passed with the stool at last. CT follow-up images on the 8th (A, D), 9th (B, E), 16th (C, F) day dynamically show the whole process of jujube pit (yellow arrows) leaving the perforation site and moving downstream spontaneously. (A-C) Jujube pit appears as a small, high-density ring on transverse images; (D-F) MPR images revealed jujube pit as a typical shuttle shape and clearly showed the relationship between jujube pit and the intestinal wall. MPR, multiplanar reconstructions; CT, computed tomography.

CT findings of perforation caused by jujube pits

The CT findings of the 11 patients with perforations are summarized in Table S4. Jujube pits piercing the intestinal wall with one sharp end or two sharp ends or jujube pits that migrated to the peritoneal space on CT directly indicated the occurrence of perforation. Indirect CT findings of intestinal perforation included thickening of the intestinal wall with abnormal enhancement, mesenteric fat stranding, localized peri-enteric gas or abscess collections, and associated intestinal obstruction. In terms of perforation sites, all 11 cases occurred in the small intestine. Except for one jujube pit perforating the duodenum, there was a subtle tendency of the perforation location to concentrate toward the terminal ileum.

Table 2 Detailed CT, endoscopic and surgical information of jujube pits from clinical cases

Parameters	Present study[†]	Reference reported[‡]	All	P value[§]
Counts of jujube pits/patients	25/22	45/45	70/67	
Size (long diameter)[¶], n (%)				–
<25 mm	7 (28.00)	–	7 (10.00)	
≥25 mm	18 (72.00)	4 (8.89)	22 (31.43)	
Not available	–	41 (91.11)	41 (58.57)	
Location of jujube pits, n (%)				0.762
Stomach	9 (36.00)	20 (44.44)	29 (41.43)	
Small intestine	13 (52.00)	22 (48.89)	35 (50.00)	
Colon	2 (8.00)	1 (2.22)	3 (4.29)	
Rectum	–	1 (2.22)	1 (1.43)	
Outside the gastrointestinal tract	1 (4.00)	1 (2.22)	2 (2.86)	
Detection of jujube pits by CT[††], n (%)				0.016*
Initial CT reports	24 (96.00)	14 (31.11)	38 (54.29)	
Increased after retrospective review	1 (4.00)	7 (15.56)	8 (11.43)	
Not available	–	24 (53.33)	24 (34.29)	

[†], there were 25 jujube pits included in present study group. [‡], a total of 45 jujube pits were included in reference reported group, including, Song *et al.*, 2021 (5), Ma *et al.*, 2021 (6), Liu *et al.*, 2020 (7), Li *et al.*, 2019 (8), Li *et al.*, 2017 (9), Lavers *et al.*, 1964 (10). [††], due to 24 patients lack related information, there were 3 articles with 21 jujube pits were compared, including Ma *et al.*, 2021 (6), Liu *et al.*, 2020 (7), Li *et al.*, 2019 (8). Therefore, the detection rate on the initial imaging reports in reference reported was 66.67%. [§], P value of comparation between present study group and reference reported group. [¶], size were not compared since size of some patients were not reported. "–", defined as the number of the relative cell is 0. "/", defined as comparation of the relative parament was not done. *, a P value of <0.05 indicates a significant difference. CT, computed tomography.

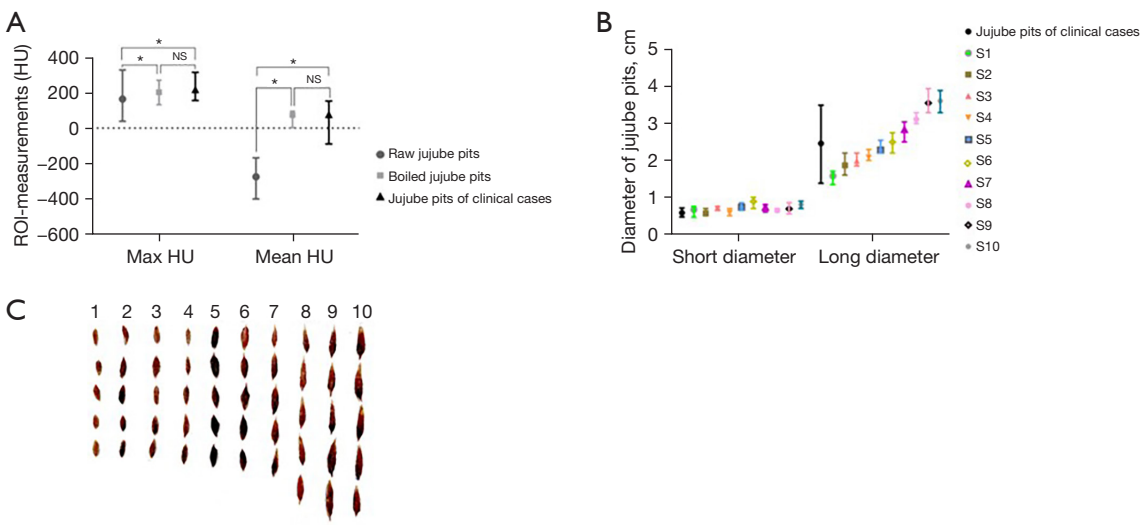

Figure 6 Comparison between CT measurements of clinically confirmed cases with the phantom results. (A) CT attenuation comparison of jujube pits from clinical cases and commercially available types in raw and boiled states. (B) size comparison of jujube pits from clinically confirmed cases and 10 commercially available types. (C) All commercially available jujube pits (10 types and five for each type) were placed on a plastic plate and further scanned with CT (in both raw and boiled state). *, a P value <0.05, indicates a significant difference. NS, not statistically significant; ROI, region of interest; CT, computed tomography.

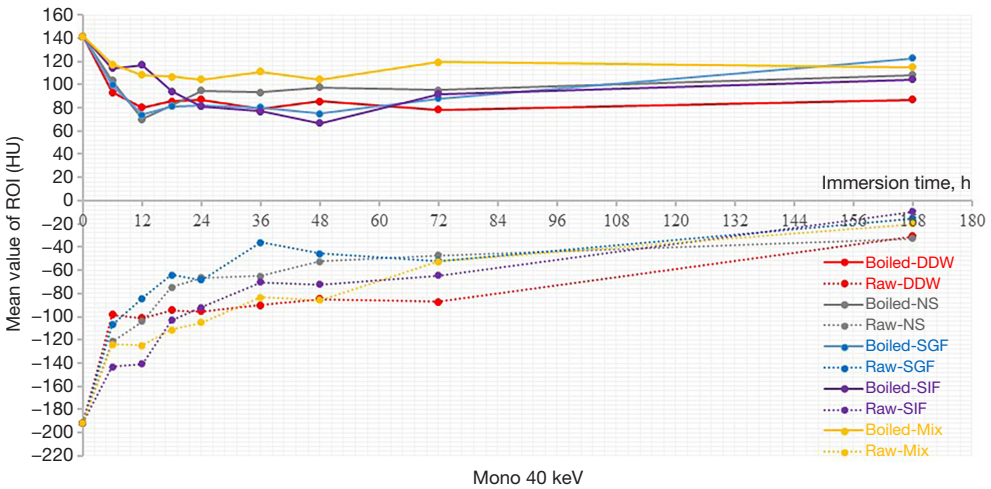

Figure 7 Mean-HUs of jujube pits with raw and boiled states immersed in different solutions against time. MIX: during the earliest 4 h, jujube pits were soaked in SGF and following that, the jujube pits were soaked in SIF mimicking human biological processes in food digestion. DDW, double distilled water; NS, normal saline; SGF, simulated gastric fluid; SIF, simulated intestinal fluid.

Ex vivo study

CT features of commercially available jujube pits

A total of 50 jujube pits were subjected to CT scans in air with raw and boiled states (*Figure 6C*). All jujube pits typically appeared as spindle-shaped along the long diameter and ring-shaped along the short diameter, with length and width of the jujube pits ranging from 1.35 to 3.95 cm and 0.4 to 1 cm, respectively (*Figure 6B*). Intra-reader agreement was excellent for length and width (ICC =0.988, P<0.001; and ICC =0.975, P<0.001, respectively). The size of the jujube pits did not change from raw to boiled.

The edge density was high, and the interior density was relatively low. However, the interior of the boiled jujube pits seemed denser as the hypodense hollow area inside was smaller or even invisible compared to the interior of the raw jujube pits. Max-HU of the raw and boiled jujube pits ranged from 39 to 329 HU and 132 to 273 HU, respectively. Intra-reader agreement was excellent for max-HU of both raw and boiled jujube pit ROIs (ICC =0.948, P<0.001; and ICC =0.958, P<0.001, respectively). The mean-HU values of the raw and boiled jujube pit ROIs were −274.28 (range: −400.12 to −168.12, SD 72.75) and 73.57 (range: 2.29 to 94.96, SD 20.48) (*Figure 6A*). Intra-reader agreement was excellent for mean-HU of both raw and boiled jujube pit ROIs (ICC =0.944, P<0.001; and ICC =0.980, P<0.001, respectively). There was a statistical difference between the mean-HU values of raw and boiled jujube pits.

Changes in jujube pits over immersion time

Neither raw nor boiled jujube pits changed in size over time. The density of raw and boiled Jujube pits varied by different degrees over time.

In the quantitative analysis of density and water content, the changing trends of mean-HU between the raw and boiled jujube pits were different. The change in the values of CT attenuation of the raw jujube pits over immersion time showed an upward trend, while the mean-HU of boiled jujube pits decreased slightly and then slightly increased (*Figure 7*). There was no statistical difference between the measurements of water content corresponding to the water-iodine and water-hydroxyapatite basis pairs. As for the structure of the jujube pits, water content ranged from high to low: high-density area of shell, slightly lower density area interior, and low-density hollow area. The percentage of blue area on water (-hydroxyapatite) images was statistically significant between raw and boiled jujube pits (50.16%±1.83% *vs.* 89.78%±0.67%, P<0.05) (*Figure 8*).

Regarding the visual assessment of density and water content, the interior density of the raw jujube pits changed over time. Based on water-hydroxyapatite material decomposition, the corresponding water overlay images enhanced the visualization of the jujube pit water content (*Figure 8*). The blue area of water (-hydroxyapatite) images showed better concordance with the relatively high-density area of conventional 120 kVp images and monochromatic 40 keV images compared to water (-iodine) images (*Figure 8*).

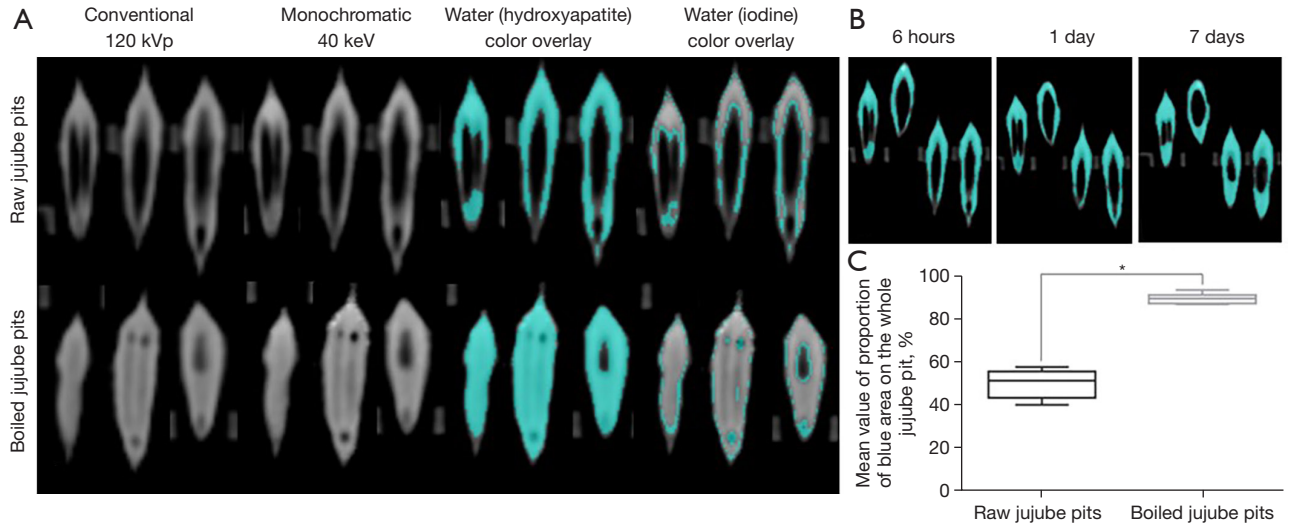

Figure 8 Changes of Jujube pits on CT images over immersion time. (A) Different sequence of three raw jujube pits (top row) and three boiled jujube pits (bottom row) in the same CT study after jujube pits immersion for 6 h. Note that the interior density varies greatly between the raw and boiled jujube pits. The blue area of water (hydroxyapatite) images shows better concordance with the high-density area of conventional 120 kVp images and monochromatic 40 keV images than water (iodine) images. (B) Water overlay images after raw jujube pits soaked for 6 h, 1 d, 7 d. The blue area expanded inward over time, while the inner hollow area shrunk. (C) Analysis of blue area percent on water (hydroxyapatite) images between raw and boiled Jujube pits. *, a P value <0.05, indicates a significant difference. CT, computed tomography.

Discussion

Jujube pits consists mainly of a hardened lignocellulosic composition and have a clear natural structure (31). The values of CT attenuation of porous materials including intraocular wooden foreign bodies and drywall change, depending on the degree of air or water content (32,33). We evaluated and analyzed the density and water content of jujube pits using dual energy-CT. Mean-HU and water content of jujube pits in raw and boiled status changed over time. While Mean-HU and water content of raw jujube pits was marked lower than boiled jujube pits. Namely, the difference in water content and density is related to the inner hollow zone. According to the above results, we speculated that its boiled or raw state and the duration of the jujube pit *in vivo* were associated with variations of the interior hypointense hollow area in the jujube pit on CT, while the location of the jujube pit was not.

In this study, water overlay images were used to reveal the changes in the water content of jujube pits. Water (-hydroxyapatite) images are used in bone diseases, as hydroxyapatite is one of the main components of bone (34). An interesting finding was that watercolor overlay images based on water-hydroxyapatite material decomposition appeared to be more appropriate for revealing changes in water content. However, more in-depth research is needed to understand whether dual energy-CT is helpful in the clinical evaluation of wooden foreign bodies.

The size of jujube pits in ex-vivo experiment and clinical cases was measured. We found that the length of the jujube pits was related to the type. Among the 10 jujube pits, the mean lengths of the four types of jujube pits were longer than or equal to 2.5 cm (*Figure 6B*). The size of the jujube pits measured by CT can be a forecasting factor for impaction and perforation. A previous study suggested that cases of sharp foreign bodies longer than 6 cm impacted in the gastrointestinal tract were more likely to undergo exploratory laparotomy than other intervention (24). Many experts pointed out that foreign bodies wider than 2.5 cm are unlikely to pass through the pylorus (12,13). In this study, the passage of the jujube pit was affected by the length and not the width. For subphrenic jujube pits (≥2.5 cm), impaction or perforation may occur. This was consistent with a previous study, which found that jujube pit longer than 2.5 cm was an independent risk factor for complications caused by esophageal jujube pit impaction (4).

Based on our cases, jujube pits may be displaced over

time after gastrointestinal perforation. The interval between preoperative CT and surgery should be as short as possible because the jujube pit may move out of its original site as seen on CT images. In the present study group, six of the patients underwent surgery within two days. Among them, the jujube pit in one patient was found to have left the original site during surgery on the second day following the CT that detected it, while this did not happen to others who underwent surgery within one day of diagnosis. This result is consistent with present study. Li *et al.* reported that four (26.67%) jujube pits were not located in the perforation sites during surgery (8). However, Li *et al.* did not provide information about the location of the jujube pits on preoperative CT and the time interval between surgery and CT.

The sensitivity of CT in detecting subphrenic jujube pits was 100% on retrospective reviews of CT images. However, a lower diagnostic sensitivity (66.7% in reference group and 96% in our group) is owing to radiologists' insufficient cognition of foreign bodies (35). According to our experience, when the long axis of the jujube pit is perpendicular to the axial plane, it appears as a small ring hence jujube pits can be easily missed or mistaken for intestinal gas content for physicians or junior radiologists. Senior radiologist can be alarmed by incidental signs of fat stranding and thickening of gastrointestinal wall. With the help of multiplanar reformation, shape of jujube pit and the relationship between sharp points and the digestive tract wall are better visualized (*Figures 3-5*), eventually the jujube pit was detected and more information can be provided for clinical management (16). Max-HU of jujube pit ROI in this study was lower than or equal to 329 HU, which can act as a threshold value to help differentiate jujube pits from other high-attenuation materials such as metal foreign bodies.

The initial diagnostic evaluation and possible treatment of ingested foreign bodies are based on the information of the ingested foreign body, subjective complaints, and clinical findings (12,36). According to our results, more than half of the participants were unable to provide relevant information of jujube pit consumption. As clinical presentations were nonspecific and lacked history of foreign body ingestion, together with reference reports, there were four (8.89%) patients who had a long course (1.5–48 months). These patients were initially treated as cases of gastroenteritis, appendicitis, tumor recurrence and perianal abscesses. Because the inflammation was secondary to jujube pit foreign bodies, the inflammation would not be completely resolved until the jujube pits were removed. If CT is used initially to assess the condition, radiologists would be the first to make an accurate diagnosis even in the absence of clinical suspicion. Thus, additional knowledge of subphrenic jujube pits and radiologist's familiarity with imaging features of jujube pit foreign objects is essential for prompt diagnosis and appropriate treatment.

There were some limitations in our study. First, the accuracy of ROI measurement can be affected by the partial volume effect and ROI, which may erroneously include voxels beyond the edge of the jujube pit. However, the intra-reader agreement was excellent for the ROI measurements. Second, the number of cases in this study was slightly low because most jujube pits are impacted in the esophagus and removed by endoscopy. But, to reflect a more comprehensive clinical situation, we conducted a comparative analysis of cases from our institution and references. And present study group included inpatients and outpatients. Third, the duration after the jujube pits impacted was not certain in most patients due to a lack of accurate diet history. This still needs a lot of clinical data and experimental support.

In conclusion, although the radiodensity of jujube pits varies greatly, CT has high sensitivity in detecting subphrenic jujube pits, as typical fusiform shaped high-density shell of jujube pits can be clearly displayed on CT images both *in vivo* and *ex vivo*. CT also plays an important role in monitoring subphrenic jujube pits.

Acknowledgments

We thank all participants and volunteers for their cooperation and efforts.
Funding: This work was supported by the Grants from the National Natural Science Foundation of China (NSFC) (Nos. 82071890, 81801695 and 82071889).

Footnote

Reporting Checklist: The authors have completed the STROBE reporting checklist. Available at https://qims.amegroups.com/article/view/10.21037/qims-22-53/rc

Conflicts of Interest: All authors have completed the ICMJE uniform disclosure form (available at https://qims.amegroups.com/article/view/10.21037/qims-22-53/coif). The authors have no conflicts of interest to declare.

Ethical Statement: The authors are accountable for all aspects of the work in ensuring that questions related to the accuracy or integrity of any part of the work are appropriately investigated and resolved. The study was conducted in accordance with the Declaration of Helsinki (as revised in 2013). Institutional ethics board of Tongji Hospital approved this retrospective cross-sectional study (No. TJ-IRB20211142), and informed consent was waived because of the retrospective nature of the study.

References

1. Gao QH, Wu CS, Wang M. The jujube (Ziziphus jujuba Mill.) fruit: a review of current knowledge of fruit composition and health benefits. J Agric Food Chem 2013;61:3351-63.
2. Li J, Shan L, Liu Y, Fan L, Ai L. Screening of a functional polysaccharide from Zizyphus Jujuba cv. Jinsixiaozao and its property. Int J Biol Macromol 2011;49:255-9.
3. Hernández F, Noguera-Artiaga L, Burló F, Wojdyło A, Carbonell-Barrachina ÁA, Legua P. Physico-chemical, nutritional, and volatile composition and sensory profile of Spanish jujube (Ziziphus jujuba Mill.) fruits. J Sci Food Agric 2016;96:2682-91.
4. Zhang X, Zhang X, Tu C, Yu Q, Fu T. Analysis of the management and risk factors for complications of esophageal foreign body impaction of jujube pits in adults. Wideochir Inne Tech Maloinwazyjne 2018;13:250-6.
5. Song JT, Chang XH, Liu SS, Chen J, Liu MN, Wen JF, Hu Y, Xu J. Individualized endoscopic management strategy for impacting jujube pits in the upper gastrointestinal tract: a 3-year single-center experience in northern China. BMC Surg 2021;21:18.
6. Ma Z, Chen W, Yang Y, Xu Z, Jiang H, Zhang Y, Lu D. Successful colonoscopic removal of a foreign body that caused sigmoid colon perforation: a case report. J Int Med Res 2021;49:300060520982828.
7. Liu YH, Lv ZB, Liu JB, Sheng QF. Perianorectal abscesses and fistula due to ingested jujube pit in infant: Two case reports. World J Clin Cases 2020;8:4930-7.
8. Li F, Zhou X, Wang B, Guo L, Ma Y, Wang D, Wang L, Zhang L, Wang H, Zhang L, Tian M, Tao M, Xiu D, Fu W. Intestinal Perforation Secondary to Pits of Jujube Ingestion: A Single-Center Experience with 18 Cases. World J Surg 2019;43:1198-206.
9. Li J, Huang H, Huo S, Liu Y, Xu G, Gao H, Zhang K, Liu T. Ectopic pancreatic tissue in the wall of the small intestine: Two rare case reports. Medicine (Baltimore) 2017;96:e7986.
10. Lavers GD, Feldmayer JE. Jujube. A case of perforated bowel. Calif Med 1964;101:206-7.
11. Lichtenstein KM, Russell TB, Lichtenstein JB, Brar HS. A date pit induced aorto-oesophageal fistula: a case report and concise literature review. Oxf Med Case Reports 2021;2021:omaa140.
12. Birk M, Bauerfeind P, Deprez PH, Häfner M, Hartmann D, Hassan C, Hucl T, Lesur G, Aabakken L, Meining A. Removal of foreign bodies in the upper gastrointestinal tract in adults: European Society of Gastrointestinal Endoscopy (ESGE) Clinical Guideline. Endoscopy 2016;48:489-96.
13. Ikenberry SO, Jue TL, Anderson MA, Appalaneni V, Banerjee S, Ben-Menachem T, Decker GA, Fanelli RD, Fisher LR, Fukami N, Harrison ME, Jain R, Khan KM, Krinsky ML, Maple JT, Sharaf R, Strohmeyer L, Dominitz JA. Management of ingested foreign bodies and food impactions. Gastrointest Endosc 2011;73:1085-91.
14. Kuzmich S, Burke CJ, Harvey CJ, Kuzmich T, Andrews J, Reading N, Pathak S, Patel N. Perforation of gastrointestinal tract by poorly conspicuous ingested foreign bodies: radiological diagnosis. Br J Radiol 2015;88:20150086.
15. Gayer G, Petrovitch I, Jeffrey RB. Foreign objects encountered in the abdominal cavity at CT. Radiographics 2011;31:409-28.
16. Guelfguat M, Kaplinskiy V, Reddy SH, DiPoce J. Clinical guidelines for imaging and reporting ingested foreign bodies. AJR Am J Roentgenol 2014;203:37-53.
17. Murray N, Darras KE, Walstra FE, Mohammed MF, McLaughlin PD, Nicolaou S. Dual-Energy CT in Evaluation of the Acute Abdomen. Radiographics 2019;39:264-86.
18. Schabel C, Patel B, Harring S, Duvnjak P, Ramírez-Giraldo JC, Nikolaou K, Nelson RC, Farjat AE, Marin D. Renal Lesion Characterization with Spectral CT: Determining the Optimal Energy for

Virtual Monoenergetic Reconstruction. Radiology 2018;287:874-83.
19. Shen H, Yuan X, Liu D, Tu C, Wang X, Liu R, Wang X, Lan X, Fu K, Zhang J. Multiparametric dual-energy CT to differentiate stage T1 nasopharyngeal carcinoma from benign hyperplasia. Quant Imaging Med Surg 2021;11:4004-15.
20. Fischer MA, Gnannt R, Raptis D, Reiner CS, Clavien PA, Schmidt B, Leschka S, Alkadhi H, Goetti R. Quantification of liver fat in the presence of iron and iodine: an ex-vivo dual-energy CT study. Invest Radiol 2011;46:351-8.
21. Peng Y, Ye J, Liu C, Jia H, Sun J, Ling J, Prince M, Li C, Luo X. Simultaneous hepatic iron and fat quantification with dual-energy CT in a rabbit model of coexisting iron and fat. Quant Imaging Med Surg 2021;11:2001-12.
22. Platon A, Becker M, Becker CD, Lock E, Wolff H, Perneger T, Poletti PA. Illegal intra-corporeal packets: can dual energy CT be used for the evaluation of cocaine concentration? A cross sectional study. BMC Med Imaging 2016;16:3.
23. Winklhofer S, Stolzmann P, Meier A, Schweitzer W, Morsbach F, Flach P, Kneubuehl BP, Alkadhi H, Thali M, Ruder T. Added value of dual-energy computed tomography versus single-energy computed tomography in assessing ferromagnetic properties of ballistic projectiles: implications for magnetic resonance imaging of gunshot victims. Invest Radiol 2014;49:431-7.
24. Zamary KR, Davis JW, Ament EE, Dirks RC, Garry JE. This too shall pass: A study of ingested sharp foreign bodies. J Trauma Acute Care Surg 2017;82:150-5.
25. Davarpanah AH, Eberhardt LW. Case 282: Fishbone Pylephlebitis. Radiology 2020;297:239-43.
26. Chen H, Wang Y, Zhou R, Li J. Migration of bamboo toothpick to liver causing paroxysmal pain. Quant Imaging Med Surg 2021;11:4667-70.
27. Ghaffarlou M, Golzari SE, Nezami N. A large asymptomatic foreign body in larynx and trachea. Quant Imaging Med Surg 2014;4:210-1.
28. Ngatchou W, Mols P, Ramadan AS, Ngassa M, Towo PY. Computer tomography imaging of an unusual cause of appendicitis: a case report. Quant Imaging Med Surg 2015;5:467-8.
29. Pouli S, Kozana A, Papakitsou I, Daskalogiannaki M, Raissaki M. Gastrointestinal perforation: clinical and MDCT clues for identification of aetiology. Insights Imaging 2020;11:31.
30. Raish M, Kalam MA, Ahmad A, Shahid M, Ansari MA, Ahad A, Ali R, Bin Jardan YA, Alshamsan A, Alkholief M, Alkharfy KM, Abdelrahman IA, Al-Jenoobi FI. Eudragit-Coated Sporopollenin Exine Microcapsules (SEMC) of Phoenix dactylifera L. of 5-Fluorouracil for Colon-Specific Drug Delivery. Pharmaceutics 2021;13:1921.
31. Gao J, Liu Y, Li X, Yang M, Wang J, Chen Y. A promising and cost-effective biochar adsorbent derived from jujube pit for the removal of Pb(II) from aqueous solution. Sci Rep 2020;10:7473.
32. Syed R, Kim SH, Palacio A, Nunery WR, Schaal S. Ex vivo model for the characterization and identification of drywall intraocular foreign bodies on computed tomography. Retina 2018;38:1432-5.
33. McGuckin JF Jr, Akhtar N, Ho VT, Smergel EM, Kubacki EJ, Villafana T. CT and MR evaluation of a wooden foreign body in an in vitro model of the orbit. AJNR Am J Neuroradiol 1996;17:129-33.
34. Ishiwata Y, Hieda Y, Kaki S, Aso S, Horie K, Kobayashi Y, Nakamura M, Yamada K, Yamashiro T, Utsunomiya D. Improved Diagnostic Accuracy of Bone Metastasis Detection by Water-HAP Associated to Non-contrast CT. Diagnostics (Basel) 2020;10:853.
35. Goh BK, Tan YM, Lin SE, Chow PK, Cheah FK, Ooi LL, Wong WK. CT in the preoperative diagnosis of fish bone perforation of the gastrointestinal tract. AJR Am J Roentgenol 2006;187:710-4.
36. Ambe P, Weber SA, Schauer M, Knoefel WT. Swallowed foreign bodies in adults. Dtsch Arztebl Int 2012;109:869-75.

Cite this article as: Hao L, Wang Q, Hu X, Li Z, Hu D, Shen Y. Utility of CT in detecting and monitoring subphrenic jujube pits: a retrospective cross-sectional study of clinical cases and *ex vivo* experiments. Quant Imaging Med Surg 2022;12(11):5114-5128. doi:10.21037/qims-22-53

Supplementary

Table S1 Published reports of patients with subphrenic jujube pits (5-10)

Parameters	Subtype	Lavers, 1964	Li, 2017	Li, 2019	Liu, 2020	Ma, 2021	Song, 2021	All
Numbers of patients		1	1	18	2	1	22	45
Clinical manifestations								
Age (year)	<6	0	0	0	2	0	NA	2
	6-18	0	0	0	0	0	NA	0
	19-50	0	0	3	0	0	NA	3
	>50	1	1	15	0	1	NA	18
Sex	Male	0	0	11	1	1	NA	13
	Female	1	1	7	1	0	NA	10
Dietary history	Awareness of jujube pit ingestion at first	0	NA	9	0	0	NA	9
	Recall of jujube ingestion after jujube pit removed	1	NA	NA	NA	NA	NA	1
Symptoms	Abdominal pain	1	1	18	0	1	NA	21
	Nausea/vomiting	0	1	14	0	1	NA	16
	Asymptomatic	0	0	0	0	0	NA	0
Duration of symptoms (day)	≤1	1	NA	NA	0	0	NA	1
	2–3	0	NA	NA	0	0	NA	0
	4–7	0	NA	NA	0	0	NA	0
	>7	0	NA	NA	2	1	NA	3
Physical signs	Fever	0	0	11	1	0	NA	12
	Abdominal tenderness	0	0	4	0	1	NA	5
	Tenderness and rebound Tenderness	1	1	14	0	0	NA	16
Laboratory findings	Elevated inflammation indicators[†]	1	1	18	0	1	NA	21
	Normal	0	0	0	2	0	NA	2
Jujube pits identified by CT, surgery or endoscopy and complications								
Location of jujube pits at first	Stomach	0	0	0	0	0	20	20
	Small intestine	1	1	18	0	0	2	22
	Colon	0	0	0	0	1	0	1
	Rectum	0	0	0	1	0	0	1
	Outside the GI tract	0	0	0	1[‡]	0	0	1
Size (Long diameter)	<25 mm	0	NA	NA	0	0	NA	0
	≥25 mm	1	NA	NA	2	1	NA	4
Perforation		1	1	18	2	1	NA	23
Treatments								
Treatments	Endoscopic removal	0	0	0	0	1	22	23
	Surgical removal	1	1	15	2	0	0	19
	Conservative treatments	0	0	3	0	0	0	3

[†], Elevated inflammation indicators: white blood cell counts, the percentages of neutrophil granulocyte, and C-reactive protein. [‡], The jujube pit was migrated from rectum. NA, not available; CT, computed tomography; GI, gastrointestinal.

https://dx.doi.org/10.21037/qims-22-53

Table S2 Detailed CT imaging parameters utilized for 22 enrolled patients

Parameter	1	2	3	4	5
Tube voltage (kV)	100-120	100-120	100-120	120	100
Tube current (mA)	Automatic	Automatic	Automatic	Automatic	Automatic
Matrix	512×512	512×512	512×512	512×512	512×512
Detector pitch	0.984:1	0.813	0.813	1.375:1	0.984:1
Reconstruction thickness (mm)	1.25	1.0	1.0	1.25	1.25
Slice interval (mm)	1.25	0.8	0.8	1.25	1.25

The corresponding serial number representing different CT scanners was displayed as follows: 1= Discovery CT750 HD, GE healthcare, Milwaukee, WI, USA; 2= AquilionOne TSX-301A; TOSHIBA, Japan; 3= Aquilion PRIME; TOSHIBA, Japan; 4= BrightSpeed; GE Healthcare, USA; 5= Optima CT660, GE Healthcare, USA. CT, computed tomography.

Table S3 Basic characteristics of 10 kinds of jujube pits

Sample ID	Trade name	Producing areas	Cultivar	weight of dried jujube fruits (g)	Long diameter of jujube pits (cm)	Short diameter of jujube pits (cm)
S1	Lelingzao	Leling	Ziziphus jujuba	3.07±0.43	1.58±0.12	0.67±0.06
S2	Jishanbanzao	Jishan	Jishan jujube	5.12 ±0.28	1.87±0.23	0.57±0.08
S3	Jinsixiaozao	Cangzhou	Ziziphus jujuba	3.46±0.35	1.99±0.13	0.72± 0.04
S4	Huizao	Ruoqiang	Huizao	4.99±0.86	2.08±0.13	0.58±0.08
S5	Jiaxiandazao	Jiaxian	Jujube dates	9.07 ±1.83	2.28±0.15	0.73±0.08
S6	Huanghetanzao	Liulin	Tanzao	7.08±1.62	2.50±0.20	0.89±0.11
S7	Hupingzao	Taigu	Huping dates	11.18±2.15	2.84±0.22	0.73±0.08
S8	Goutouzao	Yanchuan	Jujube dates	11.34±2.22	3.12±0.13	0.65±0.05
S9	Shandongdazao	Taian	Jujube dates	12.08±2.25	3.56±0.11	0.69±0.11
S10	Hetiandazao	Hetian	Jujube dates	7.69 ± 1.42	3.62±0.22	0.80±0.079

The data of weight, long diameter and short diameter are presented as mean ± standard deviation.

Table S4 CT features of 11 patients with intestinal perforation caused by jujube pits

CT features	No. (%)
Indirect signs of perforation	
Pit piercing the intestine and lodged in the intestinal wall	10 (90.9%)
Migration to parenteral	1 (9.1%)
Direct signs of perforation	
Bowel wall thickening	11 (100%)
Fat stranding	10 (90.9%)
Pneumoperitoneum	9 (81.8%)
Fluid collection	6 (54.5%)
Abscess	3 (27.3%)
Associated intestinal obstruction	6 (54.5%)

CT, computed tomography.

https://dx.doi.org/10.21037/qims-22-53

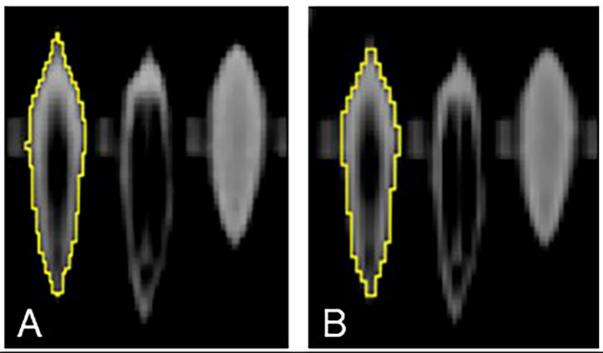

ROI	Area	Mean-HU	Min-HU	Max-HU
A	94.570	-72.479	-588	278
B	94.414	-72.141	-556	197

Figure S1 The largest section of jujube pit was marked as a ROI that was plotted along the border of jujube pit. ROI measurements were performed on monochromatic 40 keV images (A) and routine 120 kVp images (B). ROI, region of interest; HU, Hounsfield unit; Min, minimum; Max, maximum.

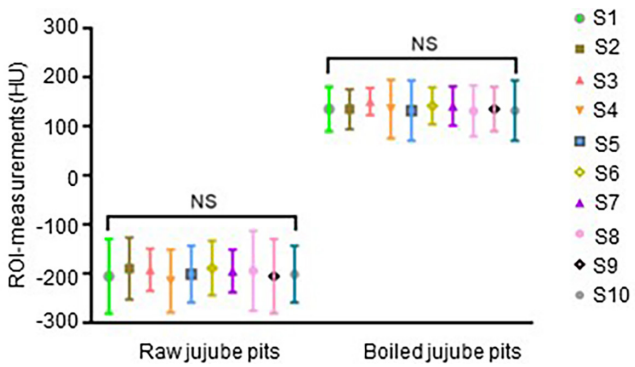

Figure S2 CT measurements of mean-HU comparing 10 commercially available types with raw and boiled states. NS, not statistically significant; CT, computed tomography, ROI, region of interest; HU, Hounsfield unit.

https://dx.doi.org/10.21037/qims-22-53